

Compensation, interstitial defects, and ferromagnetism in diluted ferromagnetic semiconductors

Georges Bouzerar,^{1,2,*} Timothy Ziman,^{2,†} and Josef Kudrnovský^{2,3,‡}

¹Laboratoire Louis Néel, 25 Avenue des Martyrs, Boîte Postale 166, 38042 Grenoble Cedex 09, France

²Institut Laue Langevin, Boîte Postale 156, 38042 Grenoble, France

³Institute of Physics, Academy of Sciences of the Czech Republic, Na Slovance 2, CZ-182 21 Prague 8, Czech Republic

(Received 31 May 2005; revised manuscript received 3 August 2005; published 23 September 2005)

We present a quantitative theory for ferromagnetism in diluted III-V ferromagnetic semiconductors in the presence of the two types of defects commonly supposed to be responsible for compensation: As antisites and Mn interstitials. In each case we reduce the description to that of an effective random Heisenberg model with exchange integrals between active magnetic impurities provided by *ab initio* calculation. The effective magnetic Hamiltonian is then solved by a semianalytical method (locally self-consistent random-phase approximation), where disorder is treated exactly. Measured Curie temperatures are shown to be inconsistent with the hypothesis that As antisites provide the dominant mechanism for compensation. In contrast, if we assume that Mn interstitials are the main source for compensation, we obtain a very good agreement between the calculated Curie temperature and the measured values, in both as-grown and annealed samples.

DOI: [10.1103/PhysRevB.72.125207](https://doi.org/10.1103/PhysRevB.72.125207)

PACS number(s): 75.50.Pp, 71.55.Eq, 72.80.Ey, 85.75.-d

Diluted magnetic semiconductors are materials where the interplay of transport and magnetic properties open the perspectives of exciting applications. The III-V semiconductors are particularly promising since a low concentration of magnetic dopants can give relatively high Curie temperatures for ferromagnetism.¹⁻⁴ In these materials it is found that the Curie temperatures depend strongly on methods of preparation and sample history; for the same nominal concentration of magnetic ions, the Curie temperature (T_C) may vary by large factors. Systematic studies show that different annealing treatments display a clear correlation between the Curie temperature and the conductivity. This indicates that the process of magnetic doping is more complex than a straight substitution [Mn(Ga)] of (formally) Ga³⁺ sites by Mn²⁺ atoms, providing a localized magnetic moment and an itinerant hole. In fact the original samples are “compensated,” i.e., the density of holes measured by transport is *lower* than the concentration of magnetic ions due to additional donor impurities, especially in the samples as grown by molecular beam epitaxy (MBE). The increase in T_C after annealing is then interpreted as removal of the defects, resulting in an increase in the hole concentration which mediates the magnetic exchange. This leaves obscure the precise form of the compensating defect, and does not provide a quantitative theory relating the Mn²⁺ concentration, the hole density, and the density of compensating defects to ferromagnetism.

There are two probable candidates for compensation: both arsenic antisites As_{Ga} (i.e., As atoms on sites of the Ga sublattice) and Mn interstitials Mn_I have long been known to be double donors. The two forms of defects differ in an important way: for each As_{Ga} there are two holes removed, i.e., only the carrier density is changed, while each interstitial, in addition, introduces a magnetic moment, changing the number of magnetically active ions. Microscopic calculations indicate that the Mn_I are preferentially situated on interstitial sites adjacent to occupied Mn(Ga) and that the coupling between interstitials and the adjacent moment is essentially given by antiferromagnetic (AF) superexchange coupling (J

≈ -320 K).⁵ In fact, there are two inequivalent interstitial positions: the Mn atom can be located inside the tetrahedron formed by either four Ga $T(\text{Ga}_4)$ or else four As $T(\text{As}_4)$. We shall make no distinction between the two possible positions sites, since in either case the AF exchange with Mn(Ga) is strongly antiferromagnetic, and we refer to Mn_I as the sum of the two.

The immediate question is, what is the proportion of the two defects, interstitials Mn_I and As_{Ga}, in the ferromagnetic samples? A conclusion of this paper is that the observed Curie temperatures in samples at different stages of annealing can *only* be explained assuming that interstitial defects dominate compensation. Such a dominance agrees with Wolos *et al.*,⁶ who estimated, from the strength of optical transitions, a relatively small (fewer than 10% of the total manganese atoms) number of antisites As_{Ga}, fewer than 10% of the total manganese atoms, and, from electron paramagnetic resonance, a much larger number of other compensating defects. Similarly Wang *et al.*⁷ showed that the saturated magnetization at low temperatures was consistent with the elimination of *two* magnetic moments with each impurity. Furthermore, polarized neutrons reflectometry⁸ and Auger spectroscopy and resistivity measurements² showed that the annealing process corresponds to redistribution of Mn sites and the increase of the magnetization far from the surface. We emphasize that clear proof of the role of interstitials is still necessary, as other techniques, by transmission electron microscopy⁹ or by infrared absorption and positron annihilation spectroscopy¹⁰ suggested a much higher concentration of antisites. The element we are bringing here is a *quantitative* theory for the Curie temperature, which as we shall explain below, is much more accurate than Zener mean-field theory. We note that in Ref. 11 we anticipated the fact that the changes in the carrier density due solely to antisites were *insufficient* to explain the reduction of T_C .

Recently, by combining first principles calculations and a semianalytical approach, we were able to provide an excellent agreement between the calculated Curie temperatures

and those measured in optimally doped semiconductors.¹¹ In the first step of this method, we derive the exchange integrals between magnetic impurities using the local density approximation (LDA) and magnetic force theorem¹² providing an effective classical random Heisenberg Hamiltonian. Note that the one particle Green's functions of the itinerant carriers used for the calculations of the calculated exchange integrals include the effect of disorder within a coherent potential approximation (CPA) for electronic motion. In the second step, we treat the random effective Heisenberg model within an approach where thermal fluctuations are treated within a self-consistent local random phase approximation (SC-LRPA), while the disorder is treated "exactly," i.e., the magnetic properties are calculated for individual configuration of disorder generated by sampling techniques. This theory is an extension of Ref. 13 where disorder in the *effective* Hamiltonian was treated by a form of CPA. An attractive feature of an "exact" treatment of disorder is that it allows us, for example, to study the effect of correlations in the disorder,¹⁴ a question of importance in interpreting experiments on high Curie-temperature samples grown using the organo-metallic vapor phase epitaxy (OMVPE) technique.¹⁵ We attribute the success of our approach to (i) the realistic calculations of the exchange integrals and (ii) to a proper treatment of the thermal fluctuations and disorder of the effective Heisenberg Hamiltonian. This second point is confirmed by consistency with Monte Carlo simulations.¹⁶

Let us now give a detailed description of the SC-LRPA. We consider the following diluted Heisenberg Hamiltonian:

$$H_{eff} = - \sum_{ij} J_{ij} \mathbf{S}_i \cdot \mathbf{S}_j. \quad (1)$$

The sum ij runs over pairs of sites occupied by the magnetic impurities (with each pair counted once). The spins are quantum with quantum number S . In the case of classical spins, we will perform properly the limit $S \rightarrow \infty$ at the end of the calculations (see below). We define the retarded Green's function,

$$G_{ij}(\omega) = \int_{-\infty}^{+\infty} G_{ij}(t) e^{i\omega t} dt, \quad (2)$$

where $G_{ij}(t) = -i\theta(t) \langle [S_i^+(t); S_j^-(0)] \rangle$.

After Tyablicov decoupling of the equation of motion of $G_{ij}(\omega)$ we obtain

$$(\omega - h_i^{eff}) G_{ij}(\omega) = 2\langle S_i^z \rangle \delta_{ij} - \langle S_i^z \rangle \sum_l J_{il} G_{lj}(\omega), \quad (3)$$

where the local effective field is

$$h_i^{eff} = \sum_l J_{il} \langle S_l^z \rangle. \quad (4)$$

For a given temperature and disorder configuration, the local magnetization $\langle S_i^z \rangle$ has to be determined self-consistently at each impurity site. In order to close the set of equations we use the Callen expression, which relate the local Green's function at site i to the local magnetization at this site,¹⁷

$$\langle S_i^z \rangle = \frac{(S - \Phi_i)(1 + \Phi_i)^{2S+1} + (S + 1 + \Phi_i)\Phi_i^{2S+1}}{(1 + \Phi_i)^{2S+1} - \Phi_i^{2S+1}}. \quad (5)$$

The expression for the local effective magnon occupation number reads

$$\Phi_i = \frac{-1}{2\pi \langle S_i^z \rangle} \int_{-\infty}^{+\infty} \frac{\text{Im } G_{ii}(\omega)}{\exp(\omega/kT) - 1} d\omega. \quad (6)$$

The previous set of equations allows us now to determine, at each temperature, the local magnetization at each impurity site and the dynamical properties such as the dynamical structure factor $S(\mathbf{q}, \omega) = (-1/\pi) \text{Im}[\sum_{ij} e^{i\mathbf{q} \cdot (\mathbf{r}_i - \mathbf{r}_j)} G_{ij}(\omega)]$.

In the vicinity of the Curie temperature, $\langle S_i^z \rangle \rightarrow 0$ the frequency integral can be simplified as the denominator can be replaced by a form linear in frequency. With a simple change of variable $E = \omega/m$,

$$\Phi_i \approx \frac{F_i k_B T_C}{m}, \quad (7)$$

where m is the total magnetization averaged over all impurity sites and

$$F_i = \int_{-\infty}^{+\infty} \frac{A_{ii}(E)}{E} dE. \quad (8)$$

The local spectral function $A_{ii}(E) = -(1/2\pi) \text{Im}[G_{ii}(E)/\lambda_i]$. In the previous equation the factor $\lambda_i = \lim_{T \rightarrow T_C} (\langle S_i^z \rangle / m)$ is determined self-consistently. Substituting the form (7) in the Callen Eq. (5) we obtain¹⁸

$$\langle S_i^z \rangle = \frac{1}{3} S(S+1) \frac{1}{\phi_i} \quad (9)$$

and

$$k_B T_C = \frac{1}{3} S(S+1) \frac{1}{N_{imp}} \sum_i \frac{1}{F_i}. \quad (10)$$

It is interesting to note that the Curie temperature can be reexpressed in terms of the eigenfunctions and eigenvalues of the following effective Hamiltonian, where the matrix elements are

$$(H_{eff})_{ij} = -\lambda_i J_{ij} + \delta_{ij} \sum_l \lambda_l J_{il}. \quad (11)$$

This leads to

$$F_i = \sum_{\alpha} \frac{| \langle i | \Psi_{\alpha} \rangle |^2}{E_{\alpha}}. \quad (12)$$

Thus the Curie temperature becomes

$$T_C^{sc} = \frac{1}{3N_{imp}} S(S+1) \sum_i \left(\sum_{\alpha} \frac{| \langle i | \Psi_{\alpha} \rangle |^2}{E_{\alpha}} \right)^{-1}. \quad (13)$$

This expression implies that the nature (for example, extended versus localized) of the eigenstate can have an important effect on the Curie temperature.

The exchange couplings calculated within first principle calculations explicitly assumed classical spins; therefore, to

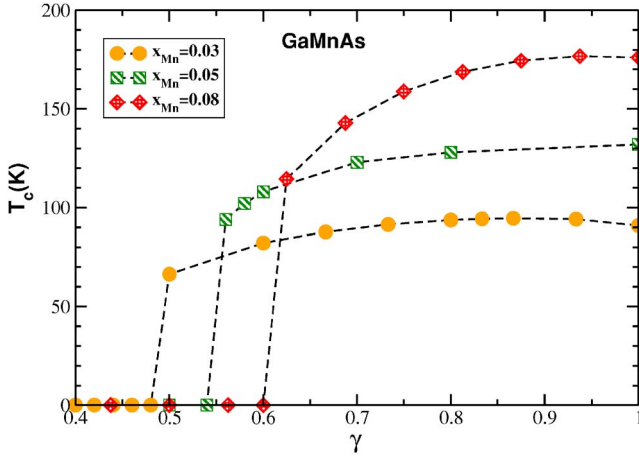


FIG. 1. (Color online) Effect of As antisites on T_C in $(\text{Ga}_{1-x_{Mn}-y_{As}}\text{Mn}_{x_{Mn}}\text{As}_{y_{As}})\text{As}$ for different Mn concentrations. The carrier density is $n_h = x_{Mn} - 2y_{As}$ and $\gamma = n_h/x_{Mn}$. The data for $x = 0.05$ are as in Ref. 11.

be consistent we must derive the Curie temperature in the classical limit. The exchange couplings which are used for the calculations are $J_{ij} = J_{ij}^{cl}/S^2$, where J_{ij}^{cl} are the couplings obtained from first principle calculations. Then we perform the limit $S \rightarrow \infty$ and find

$$k_B T_C^{cl} = \frac{1}{3} \frac{1}{N_{imp}} \sum_i F_i^{cl}, \quad (14)$$

where $F_i^{cl} = \lim_{S \rightarrow \infty} F_i/S^2$. Equation (14) will be the basis for all the results that follow.

Concluding the derivation of our theoretical method, we return to the analysis of the dependence of the Curie temperature T_C with different compensation mechanisms. First we discuss the dependence of T_C with the density of As antisites y_{As} . As in our preliminary study of this issue,¹¹ which was restricted to a single nominal concentration of Mn (5%), we do this by introducing in the *ab initio* stage of our calculation a concentration of antisites, which influences the calculated exchange couplings. As the band structure does not fix *a priori* the number of carriers, this calculation also allows us to verify, within the LDA, that there is indeed the compensation expected. In Fig. 1 we plot, for different concentration x_{Mn} of Mn, the variation of the calculated T_C in $(\text{Ga}_{1-x_{Mn}-y_{As}}\text{Mn}_{x_{Mn}}\text{As}_{y_{As}})\text{As}$ as a function of $\gamma = n_h/x_{Mn}$. Since each As antisite is a double donor, the carrier density is $n_h = x_{Mn} - 2y_{As}$. We observe that above a critical value $\gamma_c(x_{Mn})$, T_C is weakly sensitive to As antisites; this is particularly clear for $x_{Mn} = 0.03$ and 0.05. For 7% Mn, for example, we also observe that for $\gamma < 0.50$ ferromagnetism is unstable. The reason for this is that as the density decreases, the nearest neighbor exchange integral becomes increasingly dominated by the (antiferromagnetic) superexchange contribution, leading to frustration. Note also that this behavior with hole density is incompatible with Zener mean-field theory which predicts that $T_C \propto n_h^{1/3}$. Let us now discuss the compatibility of these results with the assumption that As antisites dominate the mechanism of compensation. We do this by compar-

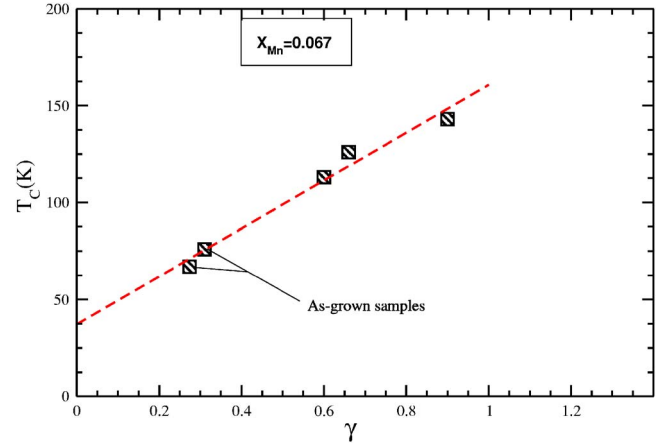


FIG. 2. (Color online) Experimental values of T_C as a function of the measured hole density per magnetic impurity $\gamma = n_h/x_{Mn}$ for $\text{Ga}_{1-x}\text{Mn}_x\text{As}$ at nominal concentration 6.7%.

ing samples with approximately fixed total density of Mn impurities but exhibiting large variation in their Curie temperatures. We plot in Fig. 2 the measured T_C^{exp} as a function of $\gamma = n_h/x_{Mn}$. In contrast to calculated values, T_C^{exp} is more sensitive to the carrier density, varying linearly with γ . The other important difference with the curves in Fig. 1 is that ferromagnetism is still observed for rather small values of γ . Thus, if we assume that As antisites dominate compensation, theory and experiment would disagree. As our approach was successful for uncompensated samples, and consistent with Monte Carlo simulations¹⁶ we conclude that As antisites do not dominate compensation.

As already mentioned, the saturated magnetization⁷ at low temperature indicates that the compensating defects affect both the density of carriers and the density of magnetically active Mn impurities. Let us now take the alternate limit in which compensation is taken to be *entirely* due to the presence of Mn interstitial defects Mn_I . We denote by x_{Mn} , $x_{Mn_{Ga}}$, and $x_{Mn(I)}$, respectively, the total density of Mn, the density of Mn on Ga sublattice, and on interstitial location, respectively. Recent first principle calculations⁵ and channeling Rutherford backscattering experiments¹⁹ indicate that Mn interstitials are preferably attracted by Mn_{Ga} and tend to form pairs of spins with strongly antiferromagnetic couplings. Thus, we suppose that Mn_I are not completely random, but are only in positions with a Mn_{Ga} as a nearest neighbor (see Fig. 3). In writing an effective Hamiltonian, we will eliminate the strongly antiferromagnetically coupled pairs of the Mn_I and adjacent Mn_{Ga} . They can be assumed, within high precision, to form bound singlet pairs whose effect on the magnetically active ions is small.²⁰ The remaining “active” Mn of density $x_{eff} = x_{Mn} - 2x_{Mn(I)}$ which are *not* directly coupled to a Mn_I , and with the measured carrier density n_h , interact via an effective Heisenberg model with couplings determined by the measured carrier density n_h . We make the same calculation as before but with the effective concentration x_{eff} and compensation γ_{eff} . Since each Mn_I is a double donor, the total density of carriers is $n_h = x_{Mn(Ga)} - 2x_{Mn(I)} = x_{Mn} - 3x_{Mn(I)}$. Thus from each measured n_h we can deduce the density of Mn_I and of “unpaired” Mn which are, respec-

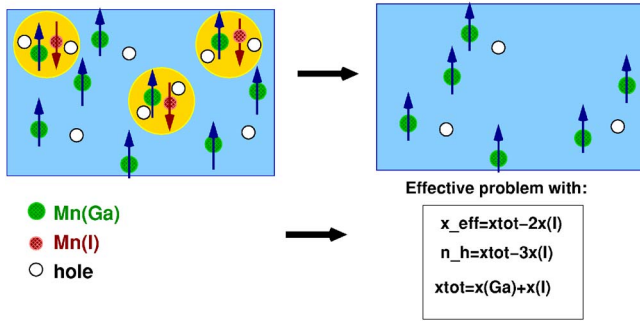


FIG. 3. (Color online) Left side: the up (down) arrows indicate spin of Mn(Ga) (Mn_I). The small circles are itinerant carrier (holes). Mn_I are double donor and strongly coupled antiferromagnetically to Mn_{Ga} . Right side: effective model with x_{eff} Mn_{Ga} impurities and n_h holes.

tively, $x_{Mn}(I) = \frac{1}{3}(x_{Mn} - n_h)$ and $x_{eff} = \frac{1}{3}(x_{Mn} + 2n_h)$. We also define the effective γ parameter as $\gamma_{eff} = n_h/x_{eff} = 3n_h/(x_{Mn} + 2n_h)$. Note that in our work we neglect effects of surface inhomogeneities^{6–8} in calculating the *bulk* ordering temperature.

In Fig. 4 we show both the experimental data² and calculated Curie temperatures. Note that for the experimental data the x axis corresponds to x_{eff} calculated for each sample using the previous expressions. Of course the nominal concentrations of each sample used in the graph are identical: 6.7%. On the same figure we note by each experimental point the ratio γ_{eff} of the measured carrier density to the effective concentration of active magnetic ions x_{eff} . As the samples have values of γ_{eff} smaller than one, for the cases of 3.5% and 5% we calculated Curie temperatures for various γ and these additional calculated points appear as filled squares

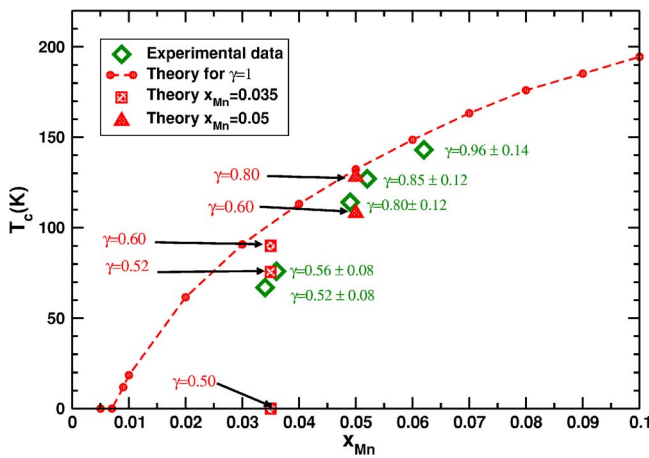


FIG. 4. (Color online) T_C for GaMnAs as a function of x_{Mn} . Note that experimental data (diamonds) are plotted as a function of x_{eff} , the density of magnetically active manganese, as explained in the text. The values of $\gamma_{eff} = n_h/x_{eff}$ corresponding to each sample are shown in the figure. The small circles, squares, and triangles are calculated Curie temperatures. The small circles (dashed line) correspond to uncompensated samples $\gamma=1$. The squares and triangles correspond to $x_{Mn}=0.035$ and 0.05 , respectively, but assumed a smaller density of holes per Mn. For these cases, the value of γ for each point is shown on the figure.

and triangles. As in Fig. 1, we vary γ in the calculations by the addition of antisites, here used as a purely calculational device to change the carrier density, while keeping the calculation fully self-consistent.²¹ The calculated points were systematically averaged over several hundred configurations of disorder and we verified that the error bars from this averaging are smaller than the plotted points. Note that some of the results corresponding to the optimally annealed sample were already published in Ref. 11, but the values have changed slightly because of improved statistics. First, we observe that the well-annealed samples (of highest T_C) are in excellent agreement with the calculated values for uncompensated samples, $\gamma=1$ curve (“optimal curve”). We remark that this optimal curve, which depends on exchange integrals recalculated for each concentration, can nevertheless be well parametrized by the simple form, up to $x_{Mn}=0.10$, $T_C \approx A(x_{Mn} - x_c)^{1/2}$ where $x_c=0.0088$, $A=649$ K for Ga(Mn)As. The samples corresponding to intermediate T_C are still in reasonable agreement with the optimal curve for uncompensated samples at the *effective* concentration of magnetically active ions. The deviation from this optimal line is small, but increasingly visible, for as-grown samples. In order to refine our calculations we have taken into account that for these samples γ_{eff} is substantially less than 1. This is why we performed additional calculations for fixed $x_{Mn}=0.035$ and 0.05 and various hole densities, as previously mentioned. We now observe that the agreement with the experimental measurements is very good for all the measured samples (as-grown and annealed). For example, the T_C as-grown sample, which corresponds to $x_{eff} \approx 0.035$ and $\gamma_{eff} \approx 0.52$, agrees very well with the calculated value (square symbol) for the same parameters. Note that using the above relations we find that the density of Mn_I in as-grown samples is $x_{Mn}(I) \approx 0.016$ which corresponds to approximately 25% of the total Mn density. This is in very good agreement with the value estimated in Ref. 22 (see Fig. 4 of that reference).

In conclusion, we have shown that experimental measurements in samples with fixed nominal magnetic impurity concentration could not be explained assuming As antisites as the dominant mechanism for compensation. On the other hand, with the assumption that Mn interstitials dominate, we obtained an excellent quantitative agreement with the measured T_C in both as-grown and annealed samples. It may be possible, in varying sample preparation, to increase the number of antisites;²³ this will have a weak effect on the T_C , provided the γ_{eff} remains above the region of instability, as seen in Fig. 1. For Ga(Mn)As samples, we can write an explicit first approximation ($\gamma_{eff}=1$) using the empirical form for the optimal curve, by replacing x_{Mn} by x_{eff} : $T_C \approx A[(x_{Mn} + 2n_h)/3 - 0.0088]^{1/2}$, where $A=649$ K. To take into account the smaller corrections due to the value of γ_{eff} we do not have an explicit analytical form, but numerical corrections can be predicted as in Fig. 1. Hence our combined *ab initio* and/or local random-phase approximation approach is a very powerful tool to study ferromagnetism in diluted ferromagnetic systems even in the presence of compensating defects. The same approach can be applied to macroscopic inhomogeneities, for example, surface effects, which may be necessary to understand thin films and devices.

We would like to thank Dr. K. Edmonds for providing unpublished additional data concerning measured critical

temperatures of (GaMn)As. We are grateful to O. Cepas and E. Kats for their comments and careful reading of the manuscript. We also thank B. Barbara, R. Bouzerar, J. Cibert, and C. Lacroix for interesting and fruitful discussions. J.K. ac-

knowledges the financial support from the grant agency of the Academy of Sciences of Czech Republic (Grant No. A1010203) and the Czech Science Foundation (Grant No. 202/04/0583).

*Email address: georges.bouzerar@grenoble.cnrs.fr or bouzerar@ill.fr

†Email address: ziman@ill.fr

‡Email address: kudrnov@fzu.cz

¹H. Ohno, *Science* **281**, 951 (1998).

²K. W. Edmonds *et al.*, *Phys. Rev. Lett.* **92**, 037201 (2004); K. W. Edmonds, K. Y. Wang, R. P. Champion, B. L. Gallagher, and C. T. Foxon, *Appl. Phys. Lett.* **81**, 4991 (2002). Additional values of T_C were provided by K. W. Edmonds *et al.* (private communication).

³S. J. Potashnik, K. C. Ku, S. H. Chun, J. J. Berry, N. Samarth, and P. Schiffer, *Appl. Phys. Lett.* **79**, 1495 (2001).

⁴T. Dietl, H. Ohno, F. Matsukura, J. Cibert, and D. Ferrand, *Science* **287**, 1019 (2000).

⁵J. Mašek and F. Máca, *Phys. Rev. B* **69**, 165212 (2004).

⁶A. Wolos, M. Kaminska, M. Palczewska, A. Twardowski, X. Liu, T. Wojtowicz, and J. K. Furdyna, *J. Appl. Phys.* **96**, 530 (2004).

⁷K. Y. Wang, K. W. Edmonds, R. P. Champion, B. L. Gallagher, N. R. S. Farley, C. T. Foxon, M. Sawicki, P. Boguslawski, and T. Dietl, *J. Appl. Phys.* **95**, 6512 (2004).

⁸B. J. Kirby, J. A. Borchers, J. J. Rhyne, S. G. E. te Velthuis, A. Hoffmann, K. V. O'Donovan, T. Wojtowicz, X. Liu, W. L. Lim, and J. K. Furdyna, *Phys. Rev. B* **69**, 081307(R) (2004); B. J. Kirby, J. A. Borchers, J. J. Rhyne, K. V. O'Donovan, T. Wojtowicz, X. Liu, Z. Ge, S. Shen, and J. K. Furdyna, *Appl. Phys. Lett.* **86**, 072506 (2004).

⁹F. Glas, G. Patriarche, L. Largeau, and A. Lemaître, *Phys. Rev. Lett.* **93**, 086107 (2004).

¹⁰F. Tuomisto, K. Pennanen, K. Saarinen, and J. Sadowski, *Phys. Rev. Lett.* **93**, 055505 (2004).

¹¹G. Bouzerar, T. Ziman, and J. Kudrnovský, *Europhys. Lett.* **69**,

812 (2005).

¹²J. Kudrnovský, I. Turek, V. Drchal, F. Maca, P. Weinberger, and P. Bruno, *Phys. Rev. B* **69**, 115208 (2004).

¹³G. Bouzerar and P. Bruno, *Phys. Rev. B* **66**, 014410 (2002).

¹⁴G. Bouzerar, T. Ziman, and J. Kudrnovský, *Appl. Phys. Lett.* **85**, 4941 (2004).

¹⁵Y. L. Soo, S. Kim, Y. H. Kao, A. J. Blattner, B. Wessels, S. Khalid, C. Sanchez Hanke, and C. C. Kao, *Appl. Phys. Lett.* **84**, 481 (2004); A. J. Blattner, P. L. Prabhuram, V. P. Dravid, and B. W. Wessels, *J. Cryst. Growth* **259**, 8 (2003).

¹⁶L. Bergqvist, O. Eriksson, J. Kudrnovský, P. A. Korzhavyi, and I. Turek, *Phys. Rev. Lett.* **93**, 137202 (2004); K. Sato, W. Schweika, P. H. Dederichs, and H. Katayama-Yoshida, *Phys. Rev. B* **70**, 201202(R) (2004).

¹⁷H. B. Callen, *Phys. Rev.* **130**, 890 (1963).

¹⁸Note that in Ref. 11 there is a factor 2 in the expression for T_C corresponding to the different definition of J_{ij} : there each exchange was counted twice in the Hamiltonian.

¹⁹K. M. Yu, W. Walukiewicz, T. Wojtowicz, I. Kuryliszyn, X. Liu, Y. Sasaki, and J. K. Furdyna, *Phys. Rev. B* **65**, 201303(R) (2002).

²⁰R. N. Bhatt and P. A. Lee, *Phys. Rev. Lett.* **48**, 344 (1982).

²¹Alternatively we found similar results by using *ab initio* rigid-band calculations, i.e., simply shifting the Fermi level by hand to tune the carrier density.

²²G. Mahieu, P. Condette, B. Grandidier, J. P. Nys, G. Allan, D. Stiévenard, Ph. Ebert, H. Shimizu, and M. Tanaka, *Appl. Phys. Lett.* **82**, 712 (2003).

²³J. Sadowski and J. Z. Domagala, *Phys. Rev. B* **69**, 075206 (2004).